ORNL/TM-13287

OAK RIDGE NATIONAL LABORATORY

LOCKHEED MARTIN

Dispersion of UO_2F_2 Aerosol and HF Vapor in the Operating Floor During Winter Ventilation at the Paducah Gaseous Diffusion Plant

S. H. Kim
N. C. J. Chen
R. P. Taleyarkhan
K. D. Keith
R. W. Schmidt
J. C. Carter

MANAGED AND OPERATED BY
LOCKHEED MARTIN ENERGY RESEARCH CORPORATION
FOR THE UNITED STATES
DEPARTMENT OF ENERGY

ORNL-27 (3-96)

ORNL/TM-13287

DISPERSION OF UO_2F_2 AEROSOL AND HF VAPOR IN THE OPERATING FLOOR DURING WINTER VENTILATION AT THE PADUCAH GASEOUS DIFFUSION PLANT

by

S.H. Kim, N.C.J. Chen, R.P. Taleyarkhan
Engineering Technology Division

K.D. Keith, R.W. Schmidt
Engineering Division

J.C. Carter
J.C. Carter Associates, Inc.

December 30, 1996

Prepared by the
Oak Ridge National Laboratory
Oak Ridge, Tennessee 37831-8045
managed by
LOCKHEED MARTIN ENERGY RESEARCH
for the
U.S. DEPARTMENT OF ENERGY
under contract DOE-840R21400

TABLE OF CONTENTS

LIST OF FIGURES

LIST OF FIGURES (Continued)

Dispersion of UO_2F_2 Aerosol and HF Vapor in the Operating Floor During Winter Ventilation at the Paducah Gaseous Diffusion Plant

1. INTRODUCTION

The gaseous diffusion process is currently employed at two plants in the United States: the Paducah Gaseous Diffusion Plant and the Portsmouth Gaseous Diffusion Plant. As part of a facility-wide safety evaluation, a postulated design basis accident involving large line-rupture induced releases of uranium hexafluoride (UF_6) into the process building of a gaseous diffusion plant (GDP) is evaluated. When UF_6 is released into the atmosphere, it undergoes an exothermic chemical reaction with moisture (H_2O) in the air to form vaporized hydrogen fluoride (HF) and aerosolized uranyl fluoride (UO_2F_2). These reactants disperse in the process building and transport through the building ventilation system.

The ventilation system draws outside air into the process building, distributes it evenly throughout the building, and discharges it to the atmosphere at an elevated temperature [1]. Outside air is drawn into the ground floor through filters by large centrifugal fans which discharge into the cell floor volume via a duct distribution system. Dampers are provided to allow flexible operation. All supply and exhaust fans are equipped with pneumatically operated dampers which close automatically when the fans are shut-down. The ventilation system in the process building is reconfigured between summer and winter months. This leads to significantly different airflow patterns during summer versus winter. During summer, the ventilation system works as a once-through system in which air is drawn into the operating floor, and then forced to the cell floor by large blowers. About 57% of air delivered to the cell floor passes through the electric motors, which drive stage compressors. This air flow is drawn by a powered exhaust system, which discharges directly to the atmosphere at roof level. The remaining air is exhausted through openings in the roof, centrally located over each cell housing. Assessments for the summer ventilation pattern have been documented elsewhere [2-4]. To prevent process gas from freezing due to low temperature during winter, the air released through motor exhaust is totally recycled between the operating and cell floors. Air from the motor exhaust duct mixes with fresh air from outside in the filter room, and is distributed throughout the operating floor (Figure 1).

Since air is recirculated from the cell floor area to the operating floor, issues concerning in-building worker safety and evacuation need to be addressed. Therefore, the objective of this study is to evaluate the transport of HF vapor and UO_2F_2 aerosols throughout the operating floor area following B-line break accident in the cell floor area.

In the postulated accident scenario, 58.97 kg/s (130 lb/s) of UF_6 vapor is released over a 10 min period from the process piping inside the cell housing, generating 30,958 kg of UO_2F_2 and 8,031 kg of HF. UO_2F_2 is assumed to remain mainly as airborne-solid particles (aerosol), whereas HF is in vapor form. Bonding between HF and water molecules in the air as well as the polymerization of HF into $(HF)_n$ are neglected in the current study for the sake of conservatism. Some UO_2F_2 particles are removed from the air flow due to gravitational settling. The HF and the remaining UO_2F_2 get mixed with air and then get exhausted through the building ventilation system.

2. METHODOLOGY

The MELCOR code was used to calculate dispersion of aerosol and vapor through the operating floor [5]. A previously developed MELCOR model for summer ventilation mode was used as a starting point [4]. A two-step approach was taken. First, an integral model combining the detailed system model developed for summer operation with a single-volume representation for the operating floor, was used to calculate transient rates of HF and UO_2F_2 mass transport into the operating floor volume. Second, using the mass rates calculated from the integral model, a separate, albeit detailed model for the operating floor volume was built to calculate spatial and temporal characteristics of aerosol and vapor transport on the operating floor area. The system model for winter ventilation mode is shown in Fig.2.

The summer ventilation model was modified to be suitable for winter ventilation of the plant. Specific modifications are:

- Motor exhausts are redirected from the environment to a corresponding operating floor volume.
- Operating floor (295.7m x 334.7m x 8.839m height) is divided into six control volumes, corresponding to each unit of the cell floor area.

- Air blowers on the cell floor area are taking air from the operating floor (since the summer model does not include the operating floor volume, air blowers were modeled to take air directly from the outside building).
- EDF (external data file) command is created to write the necessary data to be read during dispersion calculations in the operating floor.

A Detailed operating floor model has been developed. The operating floor area corresponding to units 4,5 & 6 of the cell floor area is nodalized into ten control volumes each. The remaining area is divided into three control volumes corresponding to units 1, 2 &3 of the cell floor area. A schematic of such a nodalization is shown in Figure 3. Shaded volume in the same figure, represents the operating floor volume into which UO_2F_2 and HF are sourced from the cell floor area. Two cases have been studied; one is that the aerosol and vapor are sourced into unit 4 area (case 1), and the other is that those are sourced into unit 5 area, the center region of the entire operating floor (case 2). With a separate analysis using 3x4 nodalization of each unit area of the operating floor, it was shown that air flow between units is very minimal. Therefore, it was decided to employ 1x10 nodalization for unit 4. With 1x10 nodalization for unit 4 and 1x1 nodalization for the remaining units, MELCOR predicted substantial air circulation between units, specially between units 4 and 5, which is unphysical. Pressure distribution in units 4, 5 & 6 are in parallel because these units draw a similar amount of air from the north side wall of the building. However, when unit 4 was nodalized into several volumes while units 5 & 6 were nodalized into a single volume, predictions were non-physical due to numerical problems associated with explicit coupling of flow path logic in MELCOR. Consequently, a substantial amount of air circulation was predicted in MELCOR simulation using such a nodalization scheme. Therefore, it was decided to provide same level of detail in nodalization to unit 4, 5 & 6 to prevent such an unphysical air circulation between units. Figure 4 illustrates the air flow ventilation pattern in a single unit volume of the process building. Air collected in the motor exhaust duct is expelled into the volume (e.g., filter room) near the wall. This air is mixed with air withdrawn from the outside of the building, and flows throughout the operating floor volume. Blowers located uniformly throughout the operating floor draw air from the operating floor into the cell floor area.

Vapor and aerosol mass in the operating floor are monitored to obtain their source rate into the operating floor (area corresponding to unit 4 or 5) from the cell floor area. Using control function option of MELCOR, these masses are differentiated in respect with time to yield rate of mass addition to the operating floor volume. In winter ventilation mode, air coming through the motor exhaust is mixed with air drawn from the outside building in filter rooms that are located along north- and south-side walls. This mixed air is blown into the cell floor through air blowers located throughout the operating floor area. Therefore, some fraction of HF vapor and UO_2F_2 aerosol that are drawn through motor exhaust into the operating floor, will be blown back to the cell floor. It should be noted that using the integral MELCOR model with a single volume representing the operating floor volume provides only transient results of volumetric HF and UO_2F_2 mass inventory changes. The actual time-varying mass flow rates of HF and UO_2F_2 "entering" the operating floor via motor exhaust ducts ($\dot{m}_{HF,M}$) have to be "inferred" from the volumetric quantities. This information is necessary for executing the second stage of modeling wherein spatial and temporal variations of HF and UO_2F_2 are to be evaluated on the operating floor. This value of $\dot{m}_{HF,M}$ are evaluated as follows:

$$\dot{m}_{HF,M} = \dot{m}_{HF,CV} + \dot{m}_{HF,B} \qquad (1)$$

where $\dot{m}_{HF,M}$ = rate of HF mass coming into the operating floor control volume through motor exhaust,

$\dot{m}_{HF,CV}$ = rate of HF mass inventory change in the operating floor control volume,

$\dot{m}_{HF,B}$ = rate of HF mass blown back to the cell floor area.

To evaluate $\dot{m}_{HF,M}$ from $\dot{m}_{HF,CV}$ that is a known value, we have to know a relationship between $\dot{m}_{HF,M}$ and $\dot{m}_{HF,B}$. Instead of making any significant efforts to evaluate a correct mass rate, $\dot{m}_{HF,M}$ is simply assumed to be about 33% higher than $\dot{m}_{HF,CV}$, as shown below.

$$\dot{m}_{HF,M} = 1.33\,\dot{m}_{HF,CV} \qquad (2)$$

Equation (2) indicates that $\dot{m}_{HF,M}$ can be evaluated by multiplying 1.33 to the corresponding volumetric value evaluated in the first stage. The value for UO_2F_2 mass rate can be evaluated in a similar manner. The source rate given in Eq. (2) may be underestimated . However, it must be noted that the fraction in Eq. (2) does not have any significant meaning because the main focus of this study lies in the evaluation of temporal behavior of the vapor and aerosols. Considering the uncertainty level of MELCOR modeling itself, furthermore, the absolute magnitude of the vapor and aerosol mass transport does not hold its significance because once the vapor and aerosols transport to a certain location, its magnitude is high enough to cause a significant hazard to people even with this mass source rate given in Eq. (2).

Cases 1 and 2 conservatively assume that HF vapor and UO_2F_2 aerosol are sourced into the operating floor directly either through unit 4 or 5, respectively. This means neglect of vapor and aerosol dispersion to neighboring units from the unit where vapor and aerosol are originated. In reality, vapor and aerosols should disperse to other units, and will move into corresponding unit-volumes of the operating floor through motor exhaust. Therefore, an additional case (case 3) was studied in which each unit of the operating floor volume has HF and UO_2F_2 sourced from a corresponding unit of the cell floor area. In this scenario, a pipe breakup accident to release UF_6 vapor was assumed to occur in unit 4 of the cell floor area.

3. RESULTS AND ANALYSIS

During the first stage, an integral MELCOR model was executed to generate mass source rate in a single operating floor volume, as shown in Figure 2. Using this source rate, additional MELCOR calculations were performed with detailed spatial representation of the operating floor. The first 500 seconds corresponds to the period that air flow in the operating floor reaches a steady-state condition. HF and UO_2F_2 are sourced in the operating floor starting at 500 seconds into the transient.

Results for case 1 are shown in Figures 5 through 15. In this case, HF and UO_2F_2 are sourced into the unit 4 - operating floor volume. Source rates of HF and UO_2F_2 go into the space directly below the cell floor region of unit 4 of the operating floor are plotted in Figure 5. This plot represents the rate of HF and UO_2F_2 mass changes in the unit 4 - operating floor. Therefore, a real source rate ($\dot{m}_{HF,M}$) will be numbers shown in Figure 5 multiplied by 1.33, as described by Eq. (2).

Figure 6 shows air velocity as air flows towards the middle of the building. It is seen in the figure that air drawn in the small volume near the wall keeps slowing down from about 0.45 m/s as it moves towards the middle section of the operating floor. The slowing down of air flow is mainly due to reduced air mass flow rate (as air mass keeps being depleted due to air blowers blowing air into the cell floor area). Near the middle section of the building, air velocity drops to near zero; that is almost no air flow occurs (as it should be) between unit 4 and unit 3 which is on the other side of the unit 4. One can notice that no effect of insertion of HF vapor and UO_2F_2 aerosol in air flow field is seen in the same figure. This is because MELCOR does not couple material source defined in the RN package with flow field calculation through flow-path package. However, the effects of such vapor and aerosol source to air flow stream are expected to be very small because of their small mass to be compared with air mass flow rate (~500 kg/s). The air flow velocity profile in other units is similar to that shown in Figure 6. Figure 7 shows the air velocity profile between small control volumes of unit 4 and those of unit 5 in the operating floor. As seen in the figure, cross flow values (i.e., across from major air flow field) is near zero; that is almost no flow occurs between unit volumes of the operating floor due to no modeling of turbulent mixing.

Transient variations of HF mass in the individual control volume of each unit-operating floor are shown in Figures 8 through 11. Except for unit 4 - control volumes, almost no HF vapor appears mainly because of negligible cross flow of air between unit volumes and our assumption of unit 4 as the only volume region in which HF vapor is sourced. HF vapor, as it disperses towards the middle section of the building, is depleted due to air blowers blowing HF vapor along with air into the cell floor area. HF mass starts to appear at around 900 seconds in a control volume near the middle section of the building (inner most control volume of unit 4 - cv-10). If the control room is located in cv-10, operators have about 400 seconds to evacuate from the building (900 seconds - 500 seconds of initial steady state period). Similar variations for UO_2F_2 transport are shown in Figures 12 through 15. Figure 12 shows variations of UO_2F_2 mass in control volumes of unit 4. It is seen from the curve plateaus of plots in the same figure that substantial amounts of UO_2F_2 particles are settled down on the floor. No substantial dispersion of aerosol to other units is evident from Figures 13, 14 and 15.

Results for case 2 are shown in Figures 16 through 23. In this case, HF and UO_2F_2 are sourced into the unit 5 - operating floor volume. Source rates of HF and UO_2F_2 into the unit 5 - operating floor volume are the same as those of case 1, as shown in Figure 5. Also similar air flow field is established as shown in Figures 6 and 7. Similar as the case 1, almost negligible cross flow between units is predicted. Figures 16 through 19 shows variations of HF mass in control volumes of each unit. As seen in the figures, only the control volumes of unit 5 where HF vapor is sourced have a significant HF mass. Similar to results of case 1, HF vapor takes about 400 seconds to traverse the unit (Figure 17). UO_2F_2 aerosol transport and settlement are shown in Figures 20 through 23.

Results for case 3 are shown in Figures 24 through 33. In this case, HF and UO_2F_2 are sourced appropriately into every unit of the operating floor volume. Source rates of HF and UO_2F_2 into the operating floor volume are plotted in Figures 24 and 25, respectively. Unlike plots in Figure 5 of cases 1 and 2, these plots represent motor exhaust mass flow rates of HF and UO_2F_2 sourced into the operating floor; that is, a correction was already made for a real source rate by multiplying 1.326 to rate of mass change. It is noteworthy that units 3,4 and 5 of the operating floor volume have comparable source rates even though it may be expected that the largest amount of HF vapor and UO_2F_2 aerosols should be available from unit 4 atmosphere of the cell floor area. This is because vapor and aerosols in units 3 and 5 of the cell floor area are significantly dispersed from unit 4. In unit 4 of the cell floor, a large fraction of vapor and aerosols emerging from the cell housing rises with hot plume, and escapes through the roof exhaust [4,6]. About 30% of those vapor and aerosol are sourced into unit 4 volume of the operating floor through motor exhaust. In other units of cell housing including units 3 and 5, however, no such a hot plume exists to drive vapor and aerosol towards the roof region. Consequently, much larger fraction of available vapor and aerosols can be exhausted to corresponding unit volumes of the operating floor. One can also notice from Figures 24 and 25 that onset of vapor and aerosol source into each unit of the operating floor is different. In unit 4, vapor and aerosol appear immediately after B-line breaks in one of the cell housings of unit 4 of the cell floor (500s). In other units, these plots show a time delay in the onset of vapor and aerosol source appearance, representing the time taken for vapor and aerosols in the cell floor to disperse into these units (on the cell floor). Similar air velocity profile as for cases 1 and 2 was obtained, as shown in Figures 6 and 7.

Transient variations of HF mass in the individual control volume of each unit-operating floor are shown in Figures 26 through 29. In unit 4, as seen in Figure 26, HF mass starts to appear at 500 seconds in near-wall volume (cv-1) and at 900 seconds in the middle section of the building (cv-10), similarly as cases 1 and 2. Such an appearance of vapor mass in other units is delayed because of the time taken for the vapor to disperse in other units in the cell floor area. Similar trends are shown in UO_2F_2 aerosol transport in Figures

30 through 33. Also as seen in those figures, a substantial amount of UO_2F_2 gets settled down on the floor.

Results of case 3 show that even without substantial cross flow of air between unit volumes of the operating floor, each volume will contain substantial amounts of HF vapor and UO_2F_2 aerosol that are directly exhausted from the cell floor area.

4. SUMMARY AND CONCLUSION

A two-step approach was taken to study the dispersion of HF vapor and UO_2F_2 aerosols in the operating floor. During the first stage, an integral MELCOR model was used to evaluate transient variation of the vapor and aerosol mass rate sourced into the operating floor (represented by a single control volume). Then a separate, but detailed model of the operating floor was used to investigate transient dispersion behavior of the vapor and aerosols in the operating floor. Three cases were examined. Cases 1 and 2 studied dispersion characteristics when all the vapor and aerosols were sourced into either units 4 and 5 of the operating floor, respectively. In comparison, for case 3, each unit volume of the operating floor received separate vapor and aerosol sources from the cell floor.

In all the cases, almost no dispersion of vapor and aerosol between units of the operating floor was predicted. This is mainly because of the negligible amount of bulk cross-flow of air between unit volumes. However, turbulent mixing was not possible to model using MELCOR. Turbulence may lead to additional dispersion, an aspect which should be looked into if necessary for driving more refined estimates (e.g., possibly for evacuation purposes). Also it was shown that vapor and aerosol transport to the middle section of the building where the control room is located, takes about 400 seconds. Substantial amounts of UO_2F_2 particles were predicted to settle down on the floor. When the vapor and aerosol that are already dispersed through other units of the cell floor, are sourced into each unit volume of the operating floor, substantial magnitude of vapor and aerosol are observed in units 3,4 and 5. Transport behavior of the vapor and aerosol are seen to be similar as that of cases 1 and 2.

5. REFERENCES

1. "Portsmouth Gaseous Diffusion Plant - Final Safety Analysis Report," GAT/GDP-1073, 1985.

2. S.H. Kim, et al., "Modeling And Analyses of Postulated UF_6 Release Accidents In Gaseous Diffusion Plant," ICONE-4, New Orleans, Louisiana, March 10-14, 1996.

3. S.H. Kim, et. al., "Multi-Volume Modeling and Source Term Assessment for In-Building UF6 Accidental Release in Gaseous Diffusion Plants," the 1996 Annual Summer Conference of the American Nuclear Society, Reno, Nevada, June 1996.

4. S.H. Kim, et. al.., "Source Term Evaluation for Postulated UF6 Release Accidents in Gaseous Diffusion Plants - Summer Ventilation Mode (Non-Seismic Cases)," ORNL/TM-13251, September, 1996.

5. R.M. Summers et al., "MELCOR 1.8.0: A Computer Code for Nuclear Reactor Severe Accident Source Term and Risk Assessment Analyses," NUREG/CR-5531, 1991, U.S. Nuclear Regulatory Commission.

6. M.W. Wendel, et.al. "Computational Fluid Dynamics Tracking of UF_6 Reaction Products Release into a Gaseous Diffusion Plant Cell Housing," ASME 1996 Fluids Engineering Division Summer Meeting, San Diego, CA, July 1996.

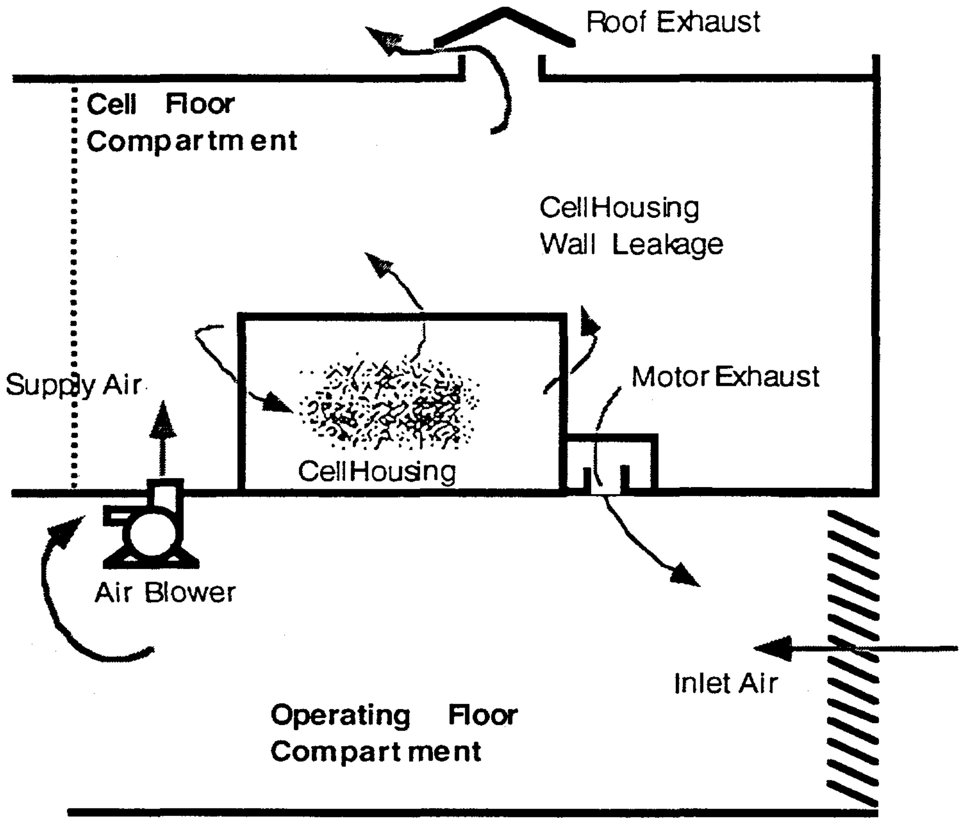

Figure 1. Winter Ventilation of Process Building at Gaseous Diffusion Plant

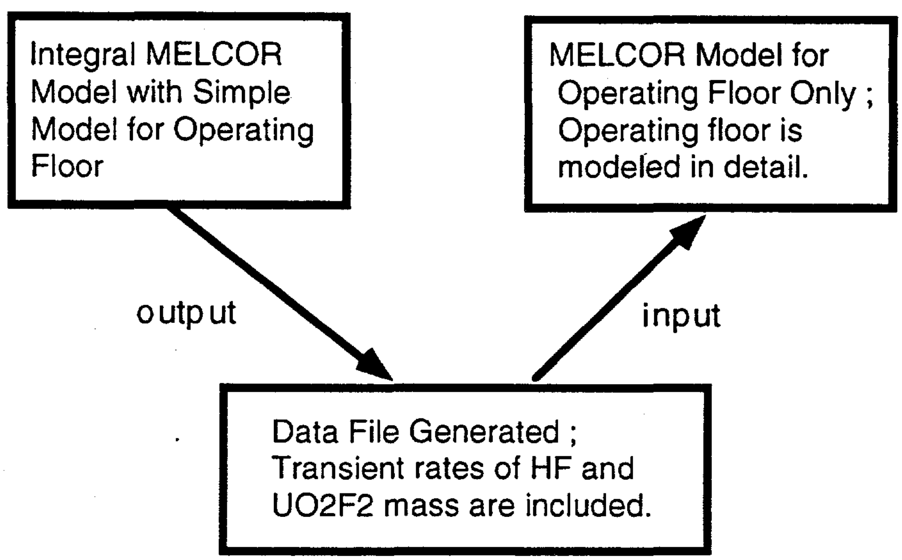

Figure 2. Two Step Approach to Study Aerosol and Vapor Dispersion in the Operating Floor

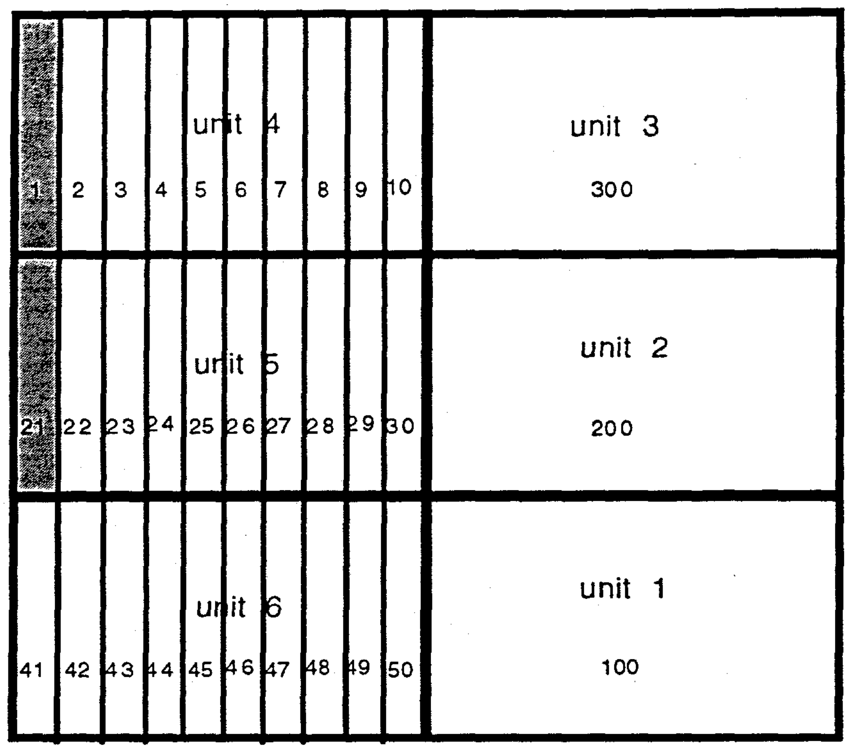

Figure 3. Nodalization of Operation Floor Volume for MELCOR Calculations; aerosol and vapor are sourced into shaded volume of unit 4 (case 1) or of unit 5 (case 2) ; Numbers represent control volume identification.

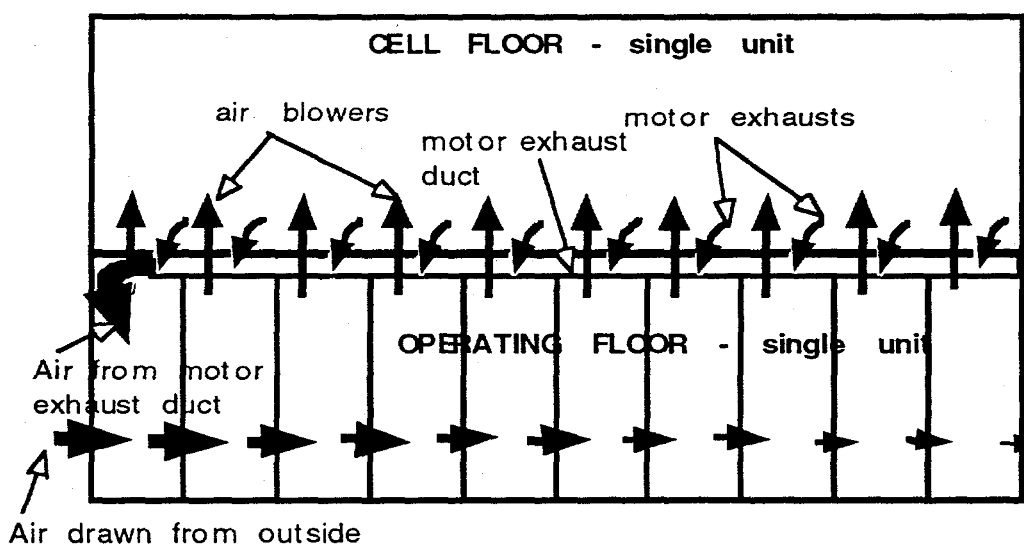

Figure 4. Air Ventilation Pattern Between Various Volumes of Process Building - One Unit of the Operating floor Is subdivided Into Ten Control Volumes (Roof exhaust is omitted in this drawing).

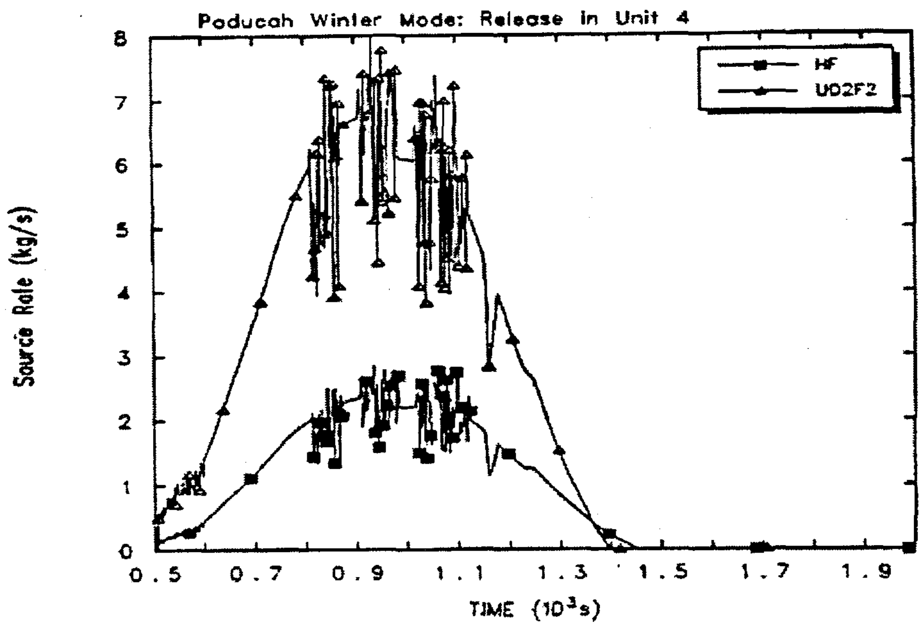

Figure 5. Rate of HF and UO_2F_2 Mass Change in the Operating Floor for Case 1

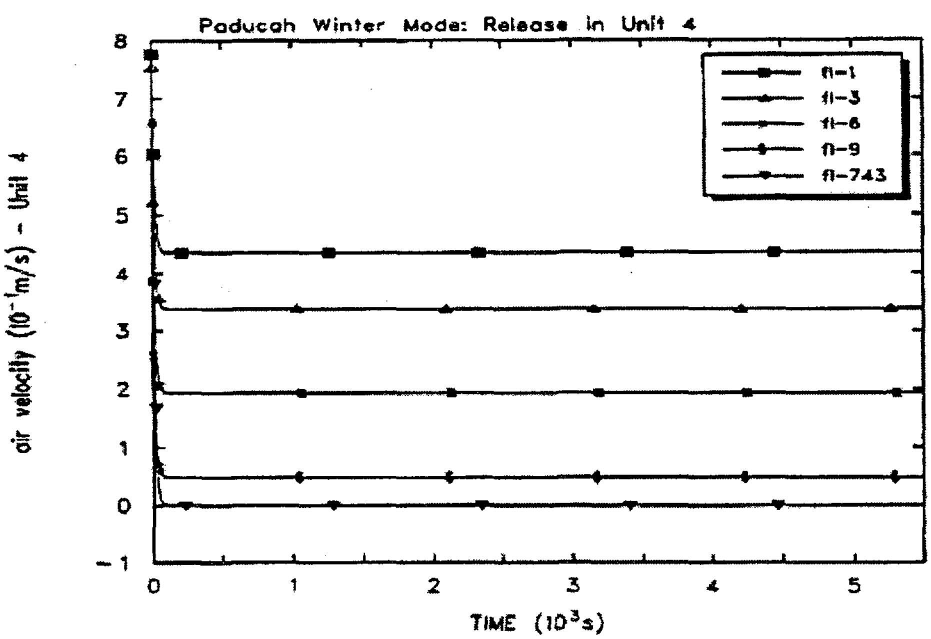

Figure 6. Inwards-Air Velocity in Unit 4 of the Operating Floor for Case 1

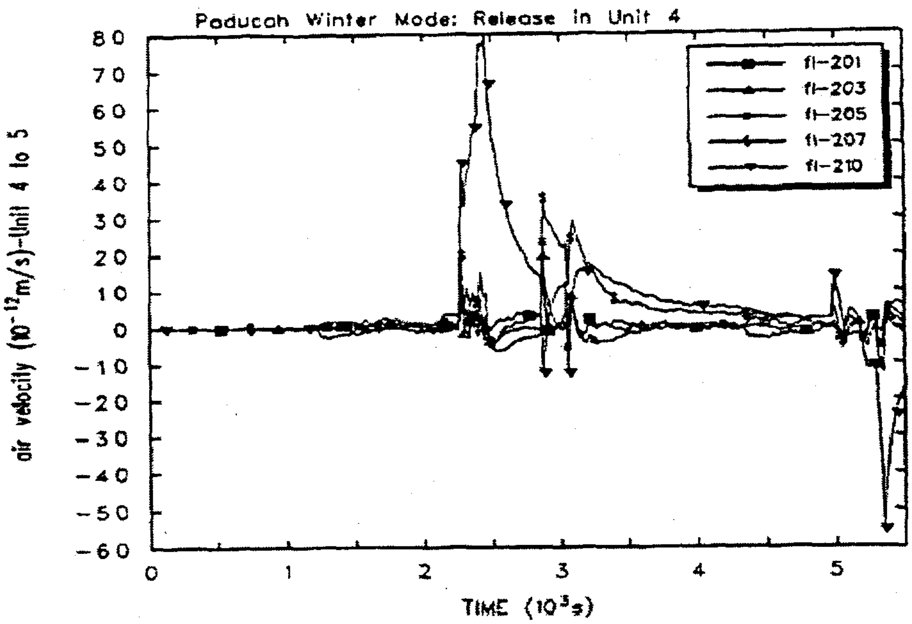

Figure 7. Air Velocity of Cross Flow Across Unit Boundaries for Case 1

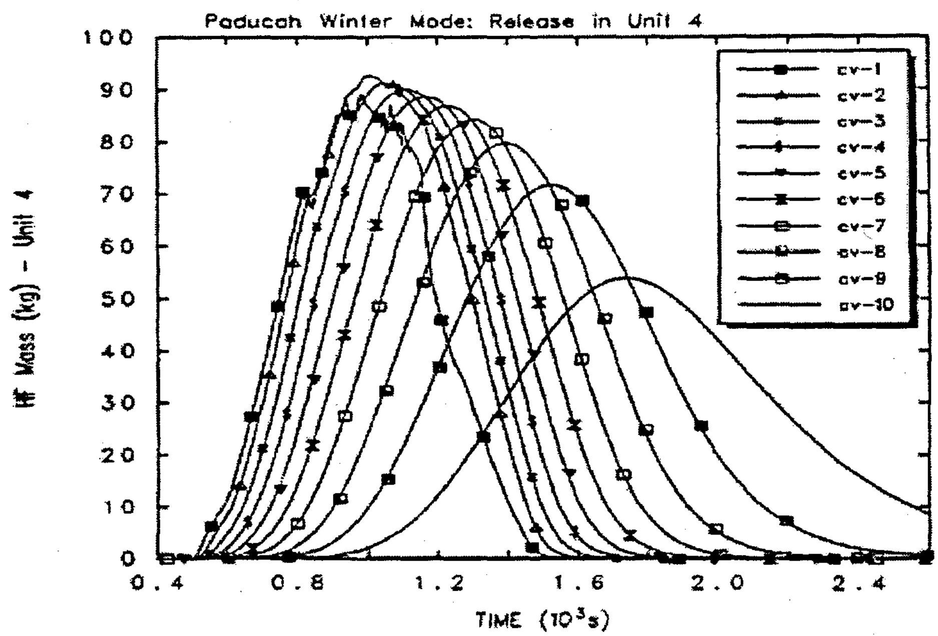

Figure 8. HF Mass Variation in Subvolumes of Unit 4 for Case 1

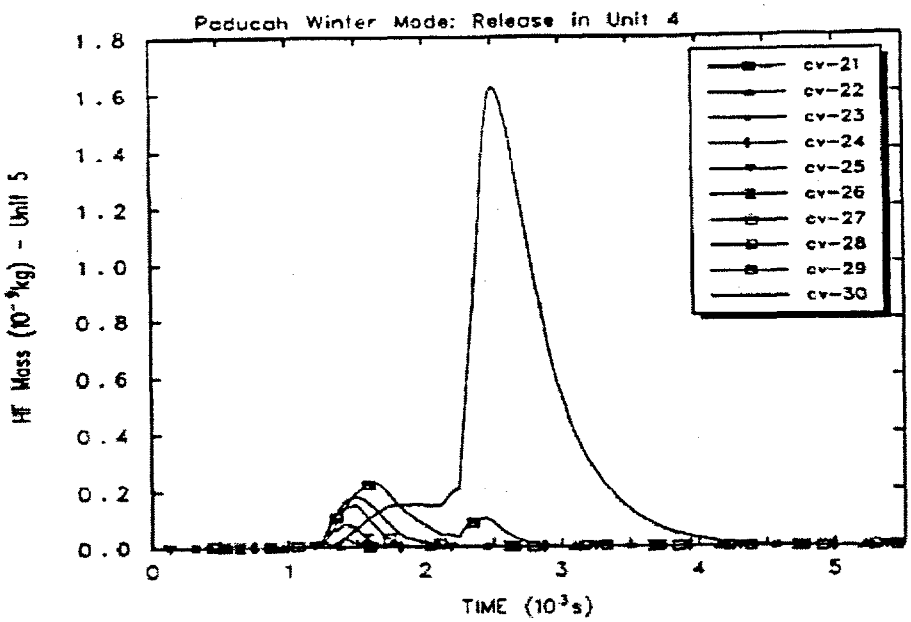

Figure 9. HF Mass Variation in Subvolumes of Unit 5 for Case 1

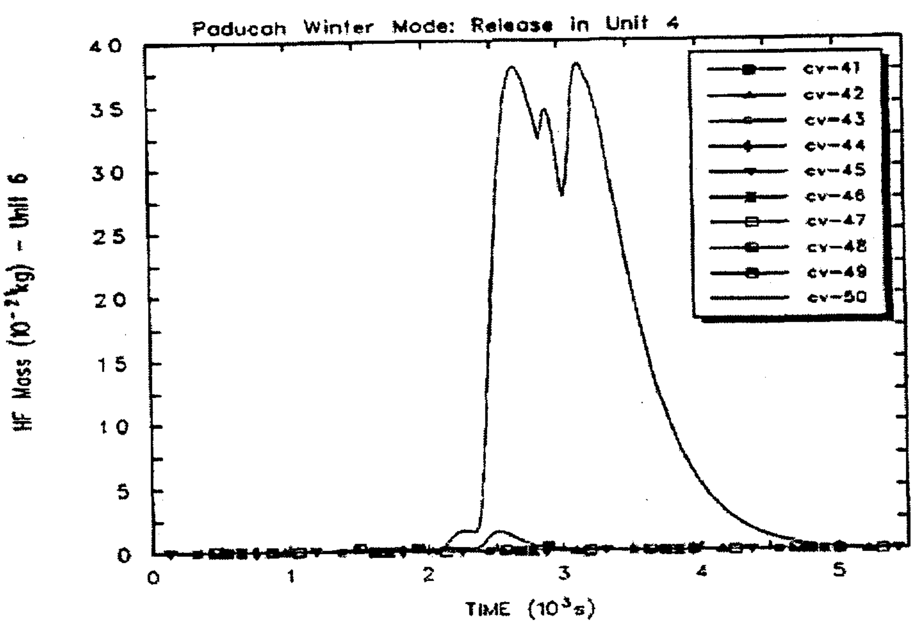

Figure 10. HF Mass Variation in Subvolumes of Unit 6 for Case 1

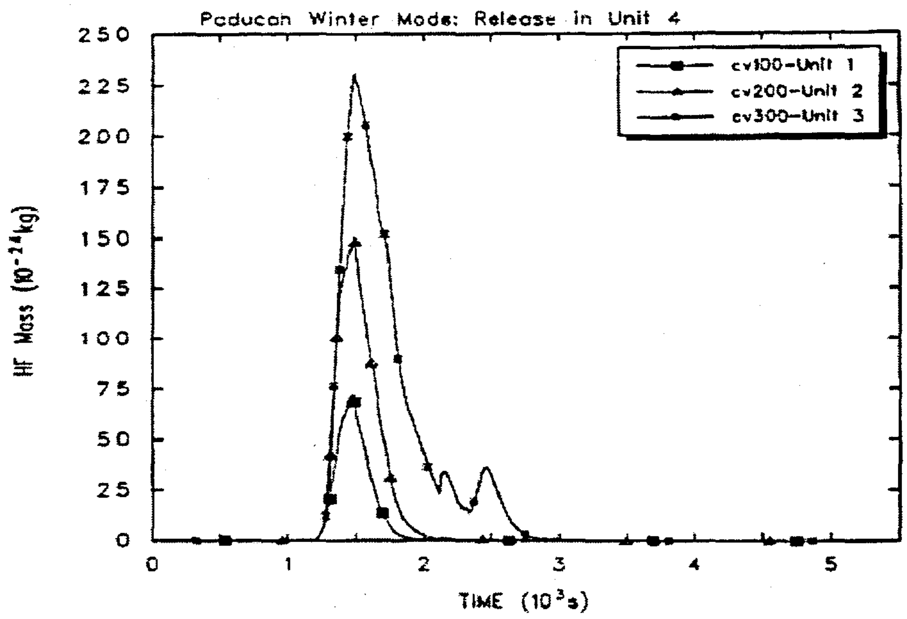

Figure 11. HF Mass Variation in Units 1,2 &3 for Case 1

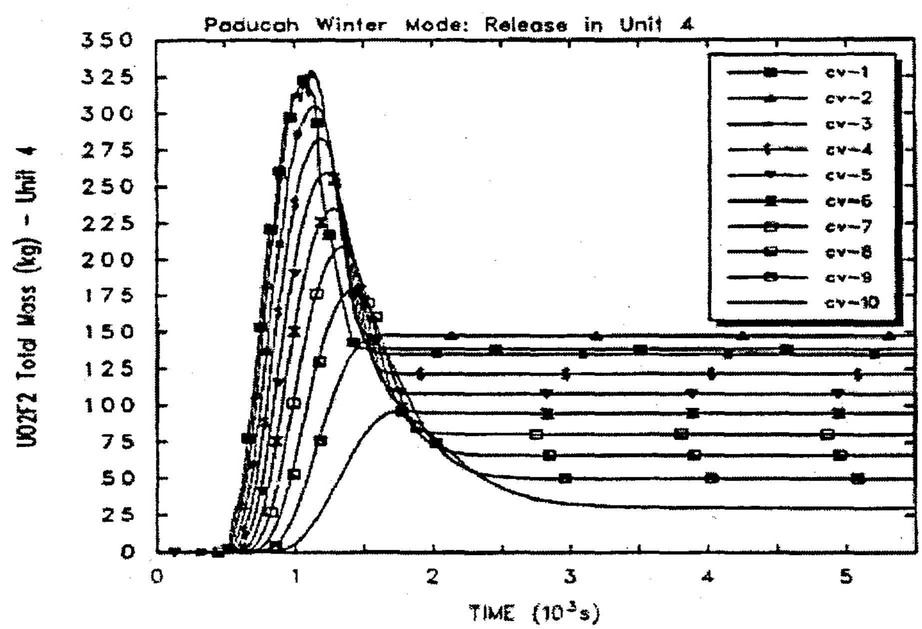

Figure 12. UO_2F_2 Mass Variation in Subvolumes of Unit 4 for Case 1

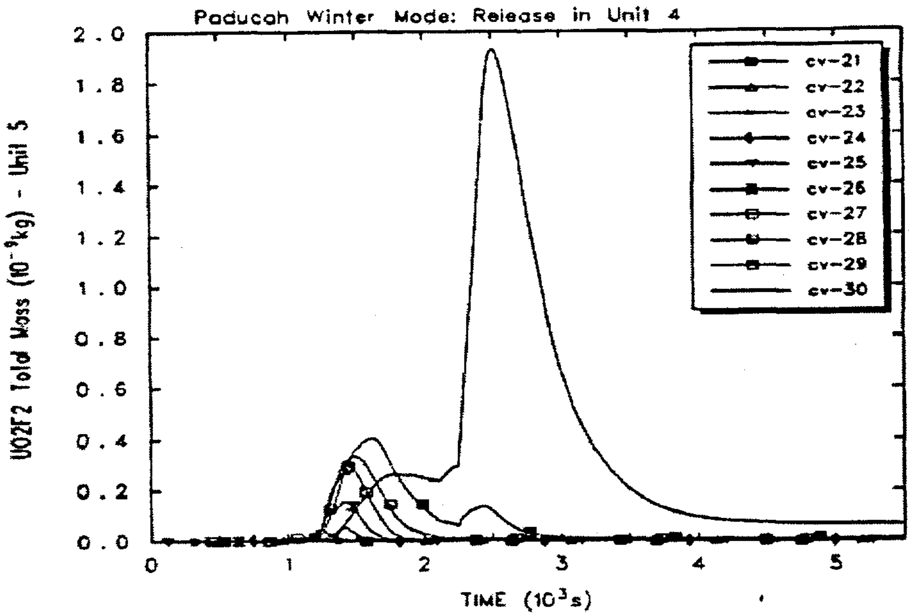

Figure 13. UO_2F_2 Mass Variation in Subvolumes of Unit 5 for Case 1

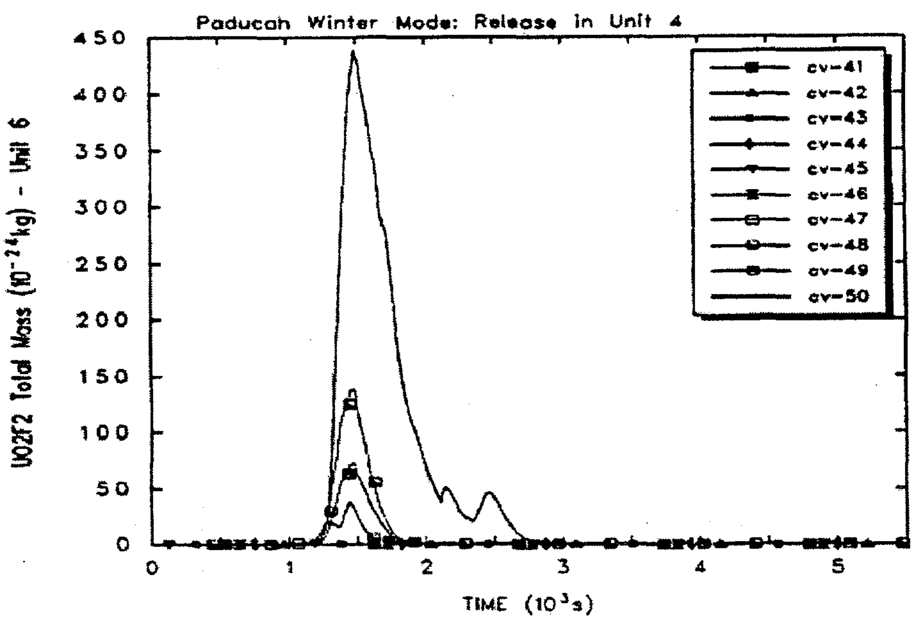

Figure 14. UO_2F_2 Mass Variation in Subvolumes of Unit 6 for Case 1

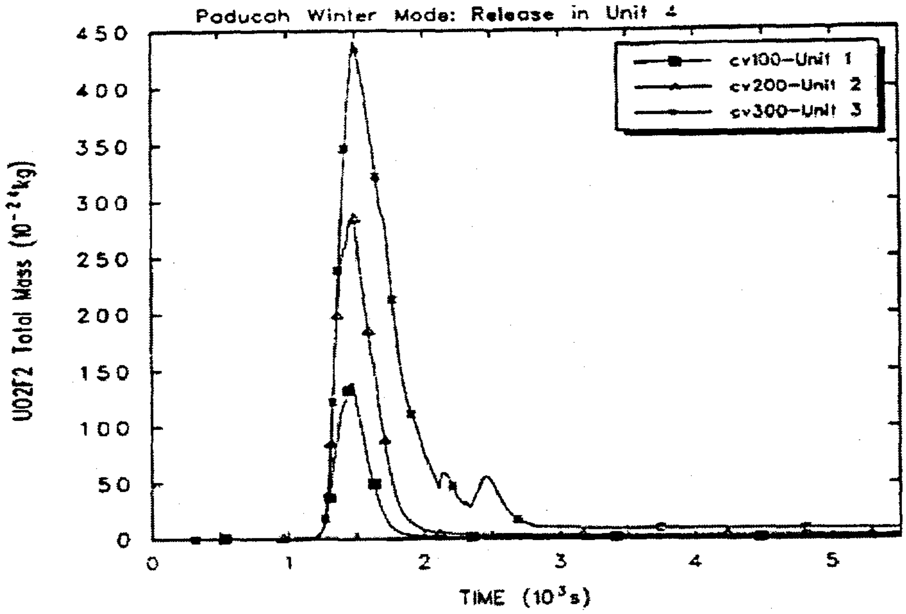

Figure 15. UO_2F_2 Mass Variation in Units 1,2 &3 for Case 1

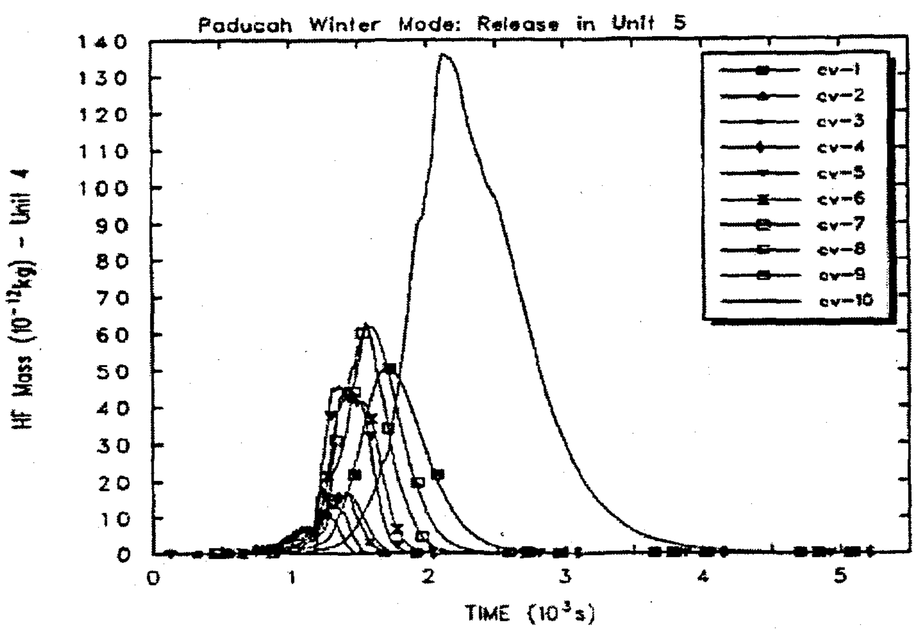

Figure 16. HF Mass Variation in Subvolumes of Unit 4 for Case 2

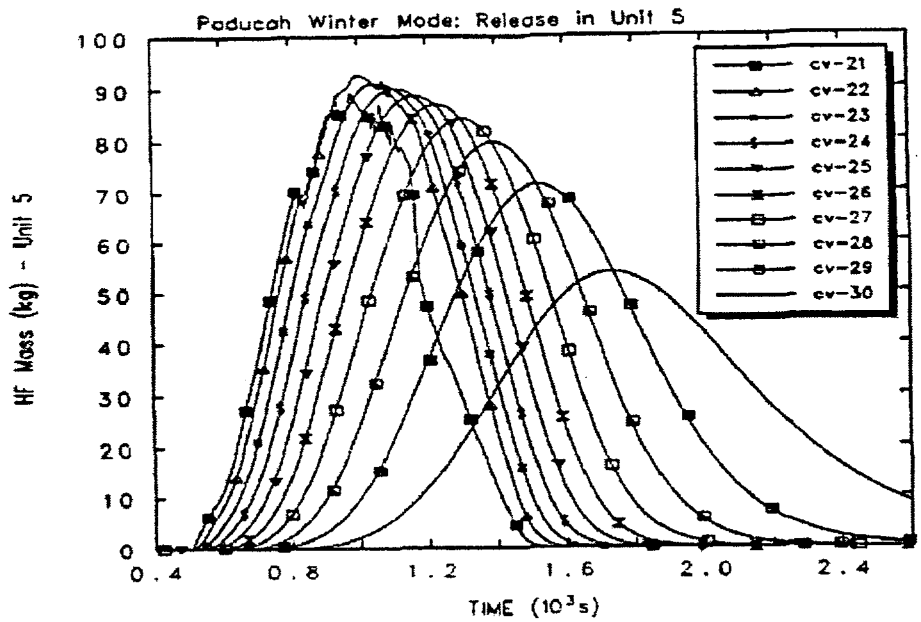

Figure 17. HF Mass Variation in Subvolumes of Unit 5 for Case 2

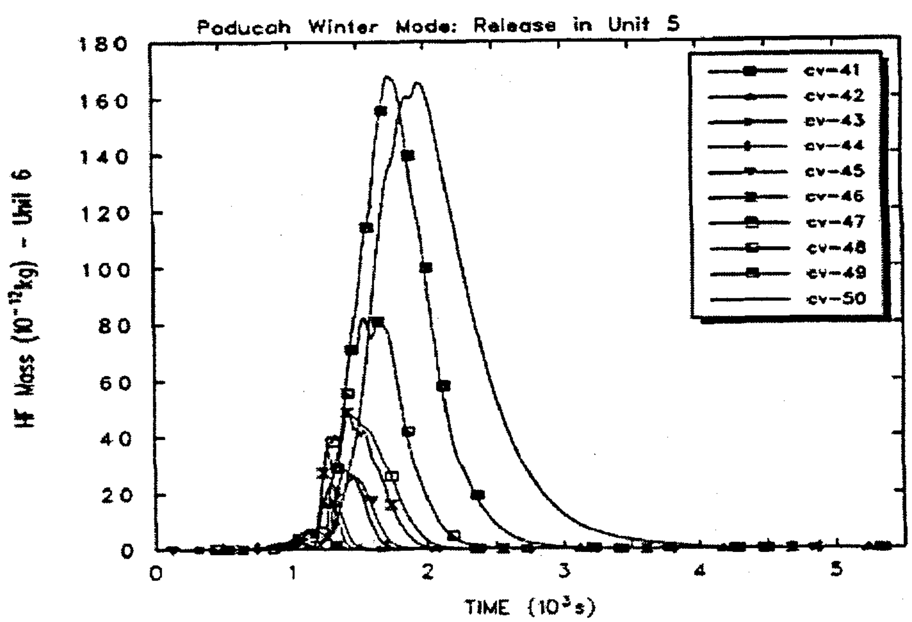

Figure 18. HF Mass Variation in Subvolumes of Unit 6 for Case 2

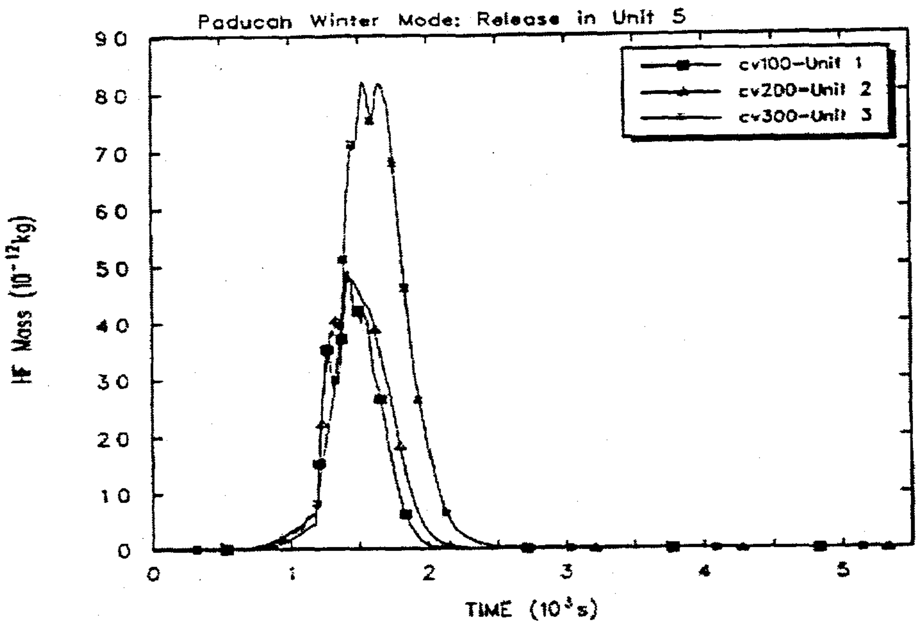

Figure 19. HF Mass Variation in Units 1,2 &3 for Case 2

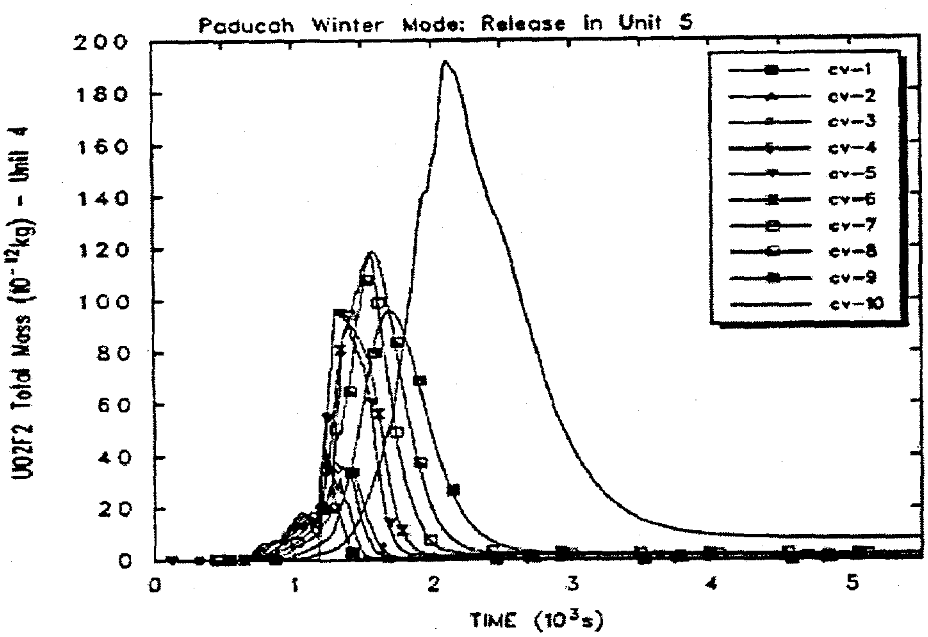

Figure 20. UO_2F_2 Mass Variation in Subvolumes of Unit 4 for Case 2

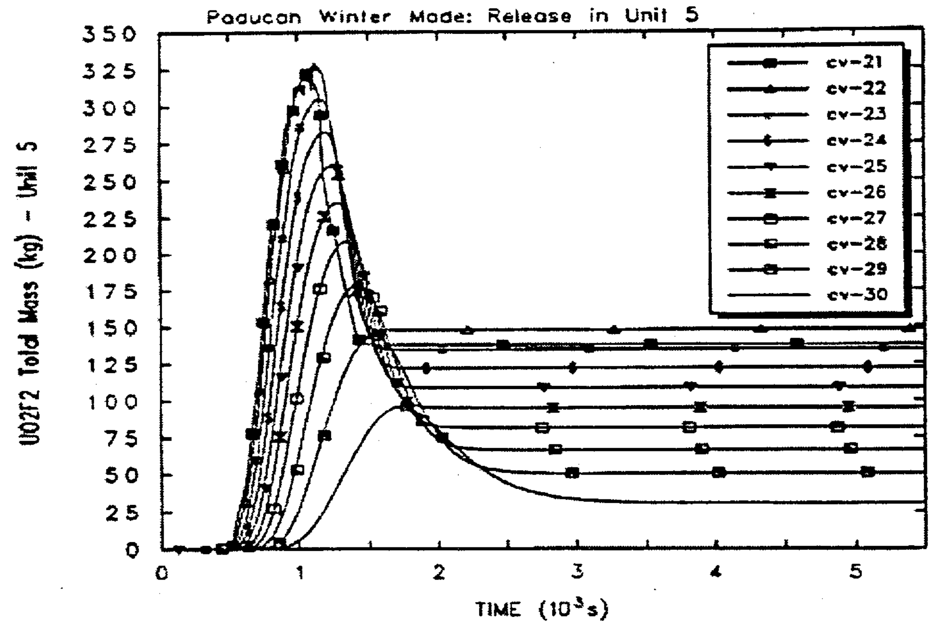

Figure 21. UO_2F_2 Mass Variation in Subvolumes of Unit 5 for Case 2

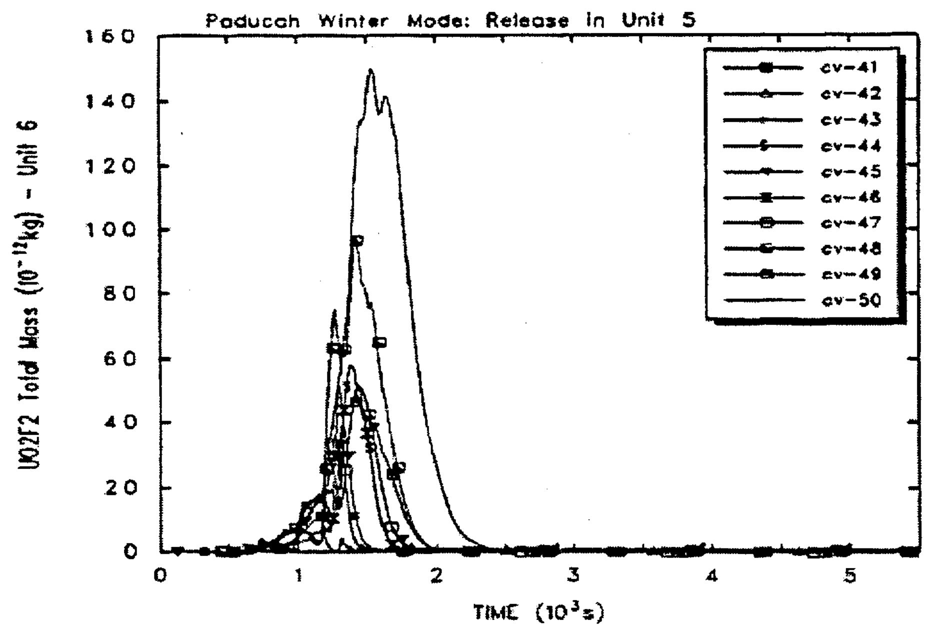

Figure 22. UO_2F_2 Mass Variation in Subvolumes of Unit 6 for Case 2

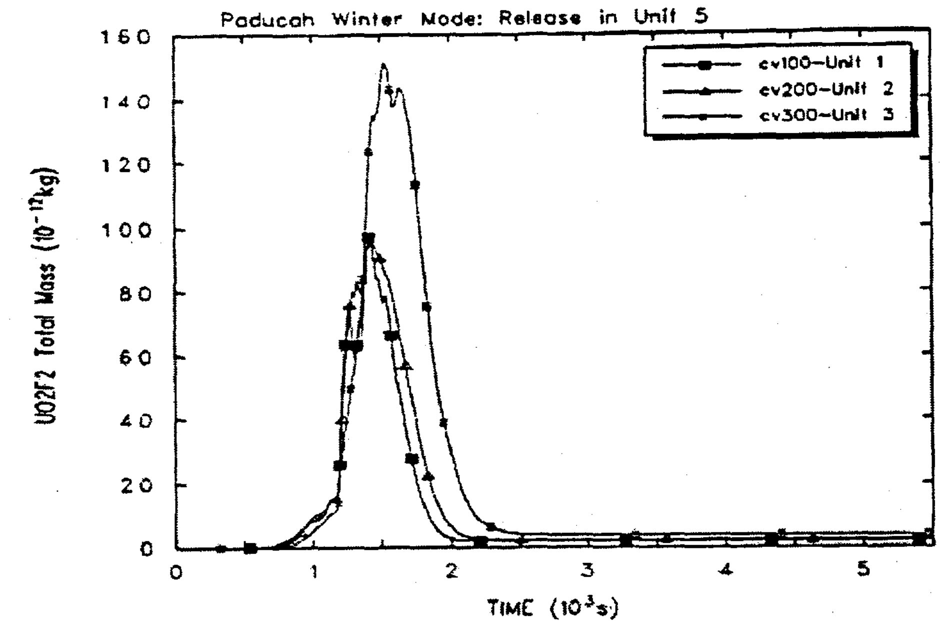

Figure 23. UO_2F_2 Mass Variation in Units 1,2 &3 for Case 2

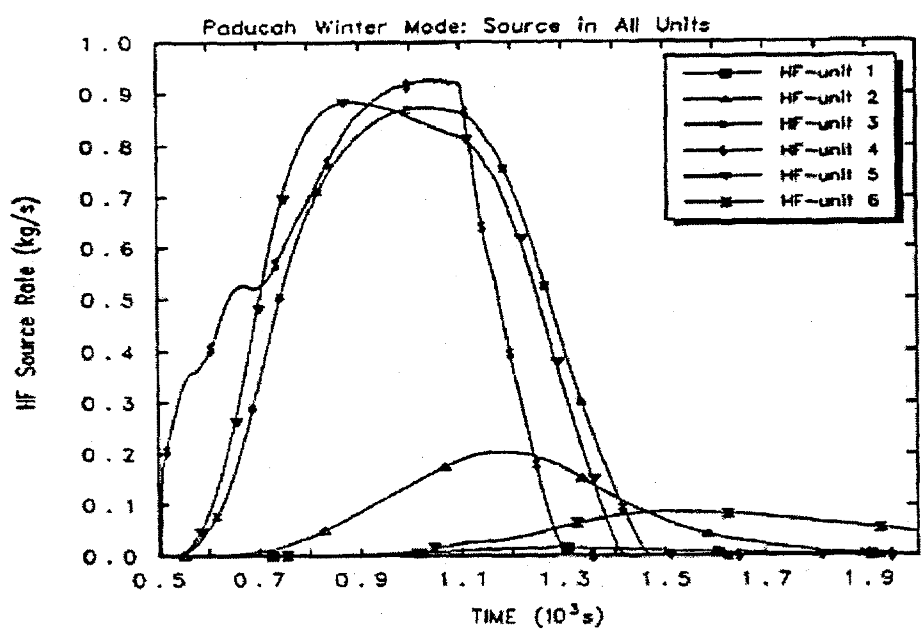

Figure 24. Rate of HF Mass Source in the Operating Floor for Case 3

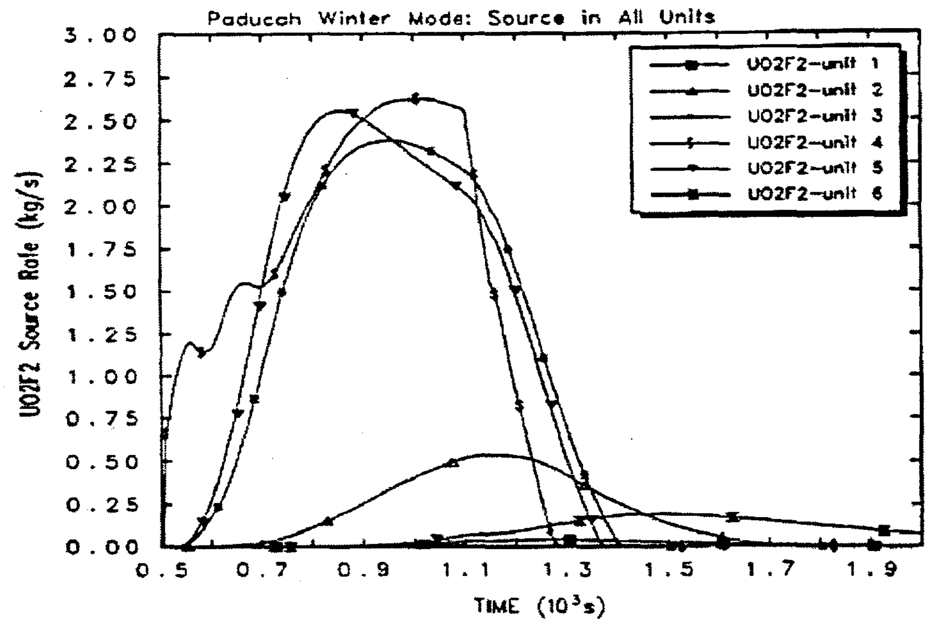

Figure 25. Rate of UO_2F_2 Mass Source in the Operating Floor for Case 3

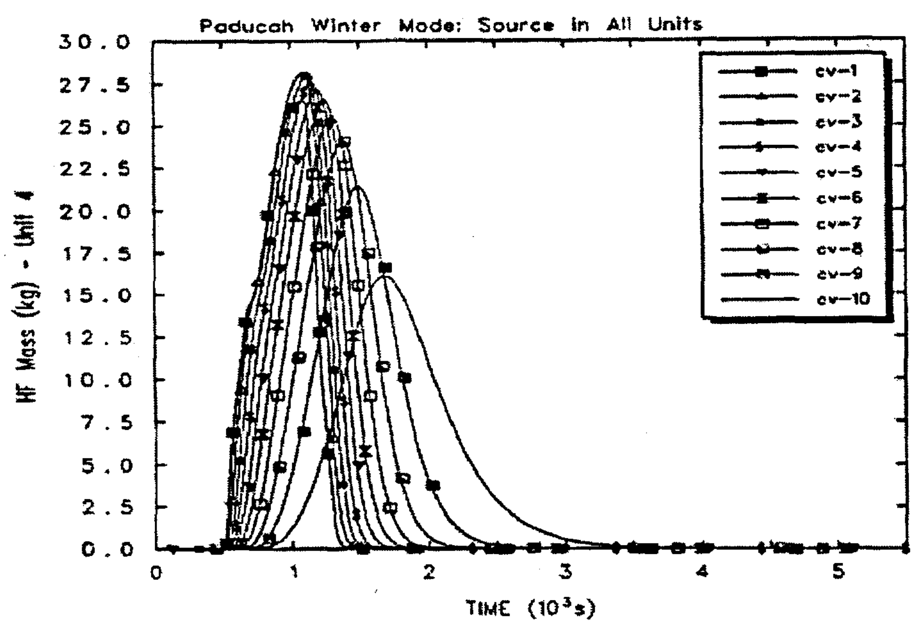

Figure 26. HF Mass Variation in Subvolumes of Unit 4 for Case 3

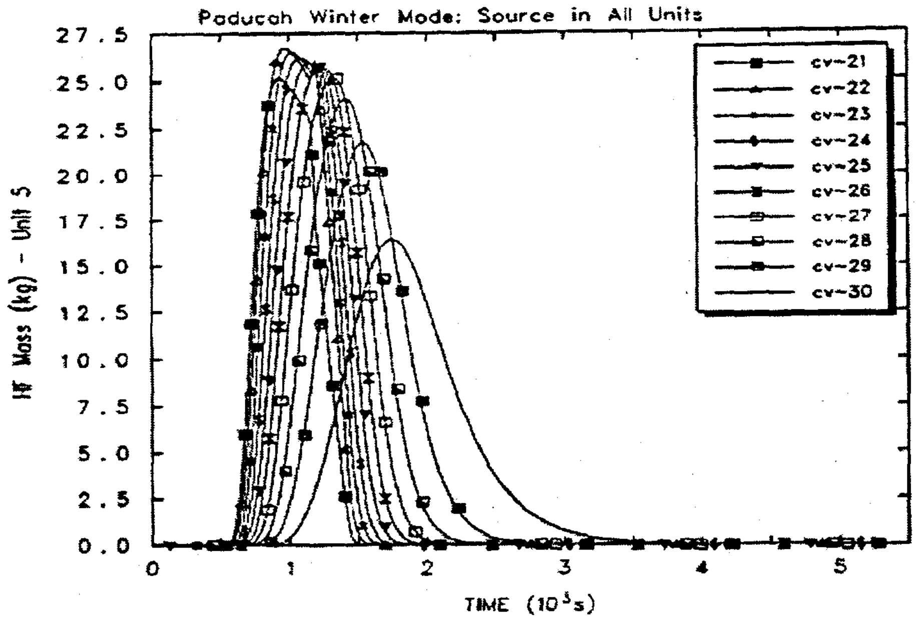

Figure 27. HF Mass Variation in Subvolumes of Unit 5 for Case 3

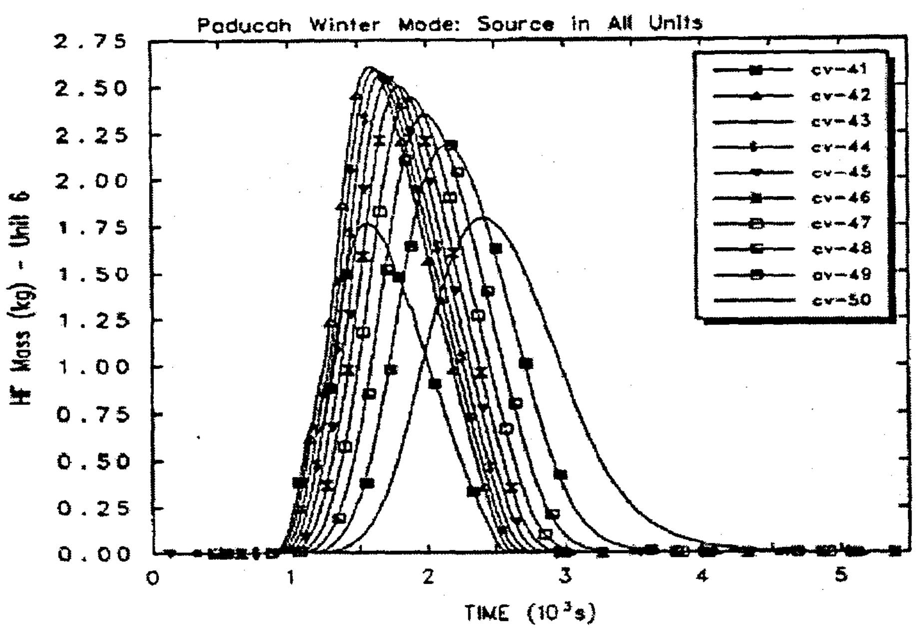

Figure 28. HF Mass Variation in Subvolumes of Unit 6 for Case 3

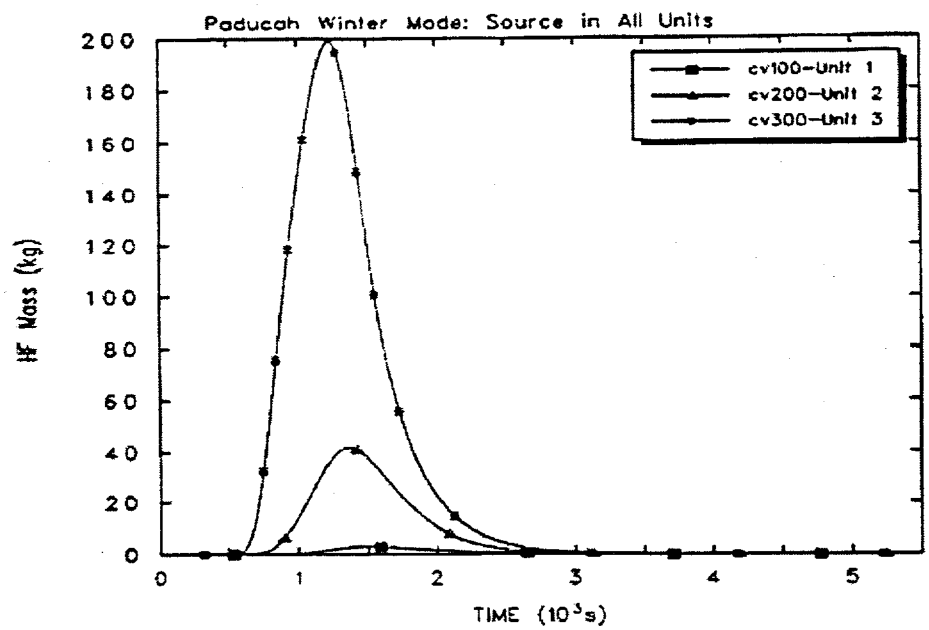

Figure 29. HF Mass Variation in Units 1,2 &3 for Case 3

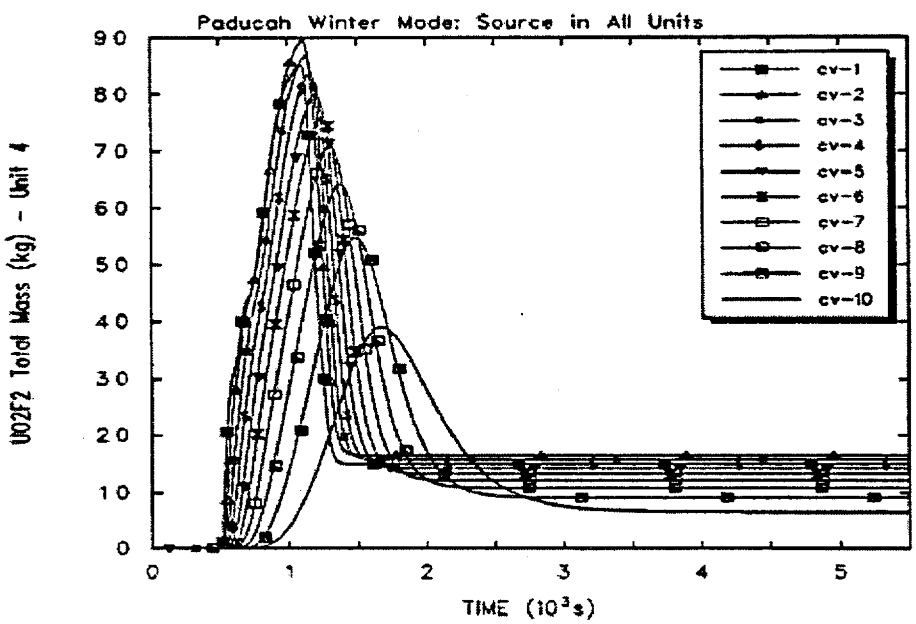

Figure 30. UO_2F_2 Mass Variation in Subvolumes of Unit 4 for Case 3

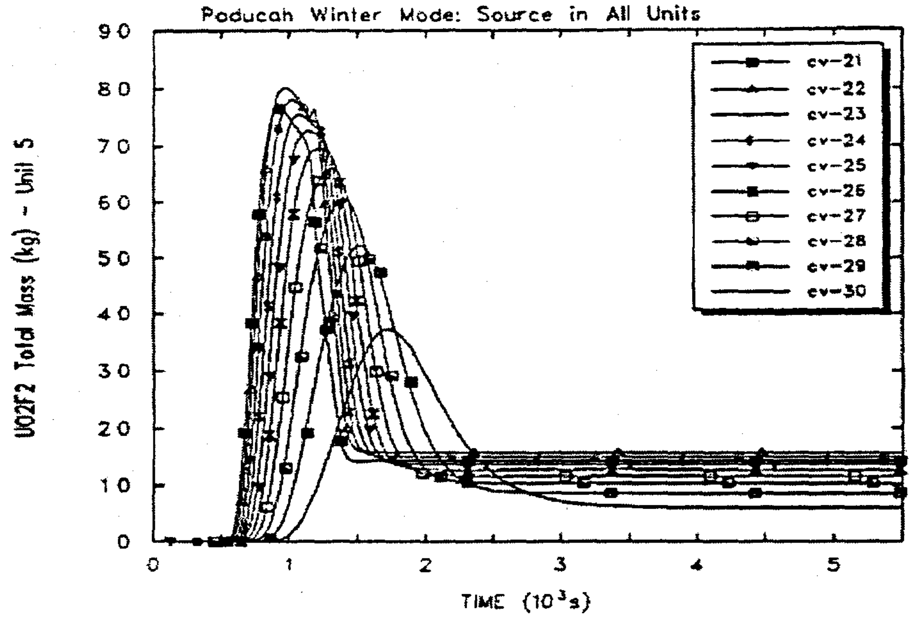

Figure 31. UO_2F_2 Mass Variation in Subvolumes of Unit 5 for Case 3

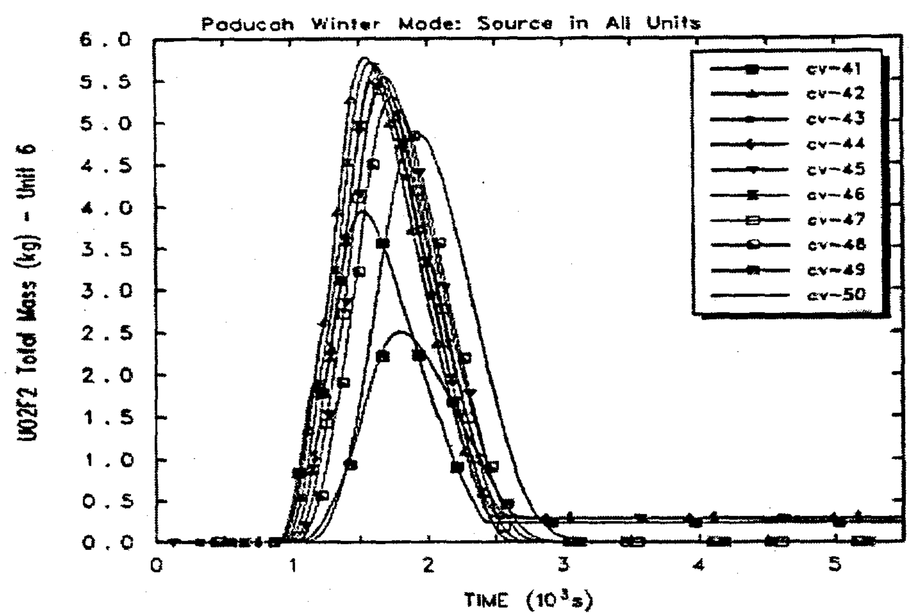

Figure 32. UO_2F_2 Mass Variation in Subvolumes of Unit 6 for Case 3

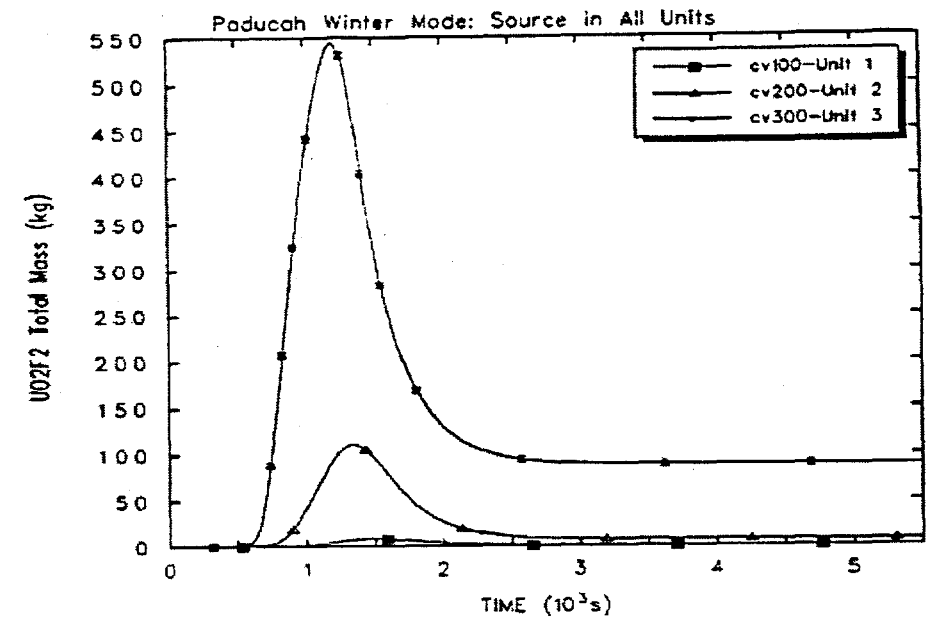

Figure 33. UO_2F_2 Mass Variation in Units 1,2 &3 for Case 3